J. Fluid Mech. (1980), *vol.* 96, *part* 2, *pp.* 335–353
Printed in Great Britain

MHD flow in a rectangular duct with pairs of conducting and non-conducting walls in the presence of a non-uniform magnetic field

By RICHARD J. HOLROYD

Department of Engineering, University of Cambridge†

(Received 10 September 1977 and in revised form 24 May 1979)

A theoretical and experimental study has been carried out on the flow of a liquid metal along a straight rectangular duct, whose pairs of opposite walls are highly conducting and insulating, situated in a planar non-uniform magnetic field parallel to the conducting walls. Magnitudes of the flux density and mean velocity are taken to be such that the Hartmann number M and interaction parameter N have very large values and the magnetic Reynolds number is extremely small.

The theory qualitatively predicts the integral features of the flow, namely the distributions along the duct of the potential difference between the conducting walls and the pressure. The experimental results indicate that the velocity profile is severely distorted by regions of non-uniform magnetic field with fluid moving towards the conducting walls; even though these walls are very good conductors the flow behaves more like that in a non-conducting duct than that predicted for a duct with perfectly conducting side walls.

1. Introduction

The main theme of this paper is a theoretical and experimental study of the steady flow of a liquid metal along a straight rectangular duct with a pair of non-conducting walls and a pair of electrically isolated conducting walls which are parallel to the field lines of a planar non-uniform magnetic field (see figure 1). This field comprises two adjacent regions of parallel uniform field of strengths B_0 and $\frac{1}{2}B_0$, the change being affected over a short length of the duct where the field is non-uniform. Magnitudes of the mean velocity V and B_0 are taken to be such that the Hartmann number M and interaction parameter N are large so that the flow can be treated as being inviscid and inertialess and the magnetic Reynolds number $R_m \ll 1$ while the conductance ratio Φ = conductance of walls/conductance of fluid (in a plane parallel to B_0 and perpendicular to V) is large but finite.

Shercliff (1962, §§ 2.3.3 and 3.3.3) examined the effects on the flow of a magnetic field whose strength increased from zero to a uniform value along the duct over a short length when both N and Φ were small. He showed that a recirculating current flow is set up in and *immediately upstream and downstream* of the non-uniform field region, part of it flowing along the conducting walls.‡ Inertial, rather than viscous, stresses

† Present address: Department of Engineering Science, University of Oxford.

‡ His results are only qualitatively correct because his analysis contains an error; the correct solution was derived by Vasil'ev & Lavrent'ev (1969).

0022-1120/80/4366-8170 $02.00

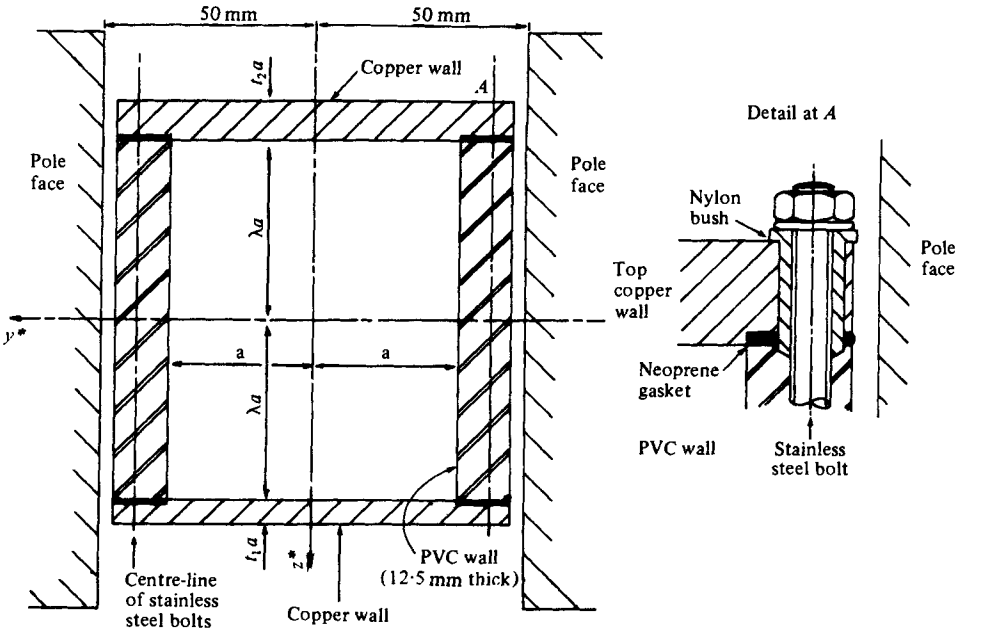

FIGURE 1. The experimental duct; $a = 34{\cdot}75\,\text{mm}$, $\lambda a = 43{\cdot}65\,\text{mm}$ ($\lambda = 1{\cdot}256$), $t_1'a = 6{\cdot}35\,\text{mm}$ ($t_1' = 0{\cdot}182$), $t_2'a = 9{\cdot}525\,\text{mm}$ ($t_2' = 0{\cdot}274$), $L'a = 1440\,\text{mm}$ ($L' = 41{\cdot}41$). Detail of corner A shows how bolts were insulated from the conducting wall thereby eliminating short circuit with the other conducting wall. End faces of pole pieces of magnet producing a region of high strength uniform field are indicated.

play an important role in determining the behaviour of the fluid. In the non-uniform field region the streamlines move towards the conducting walls regardless of the direction of the mean flow such that fractional perturbations of the streamwise velocity profile are $O(N/10)$.

Apart from the obvious differences in the values of N and Φ from those considered here, Shercliff's work differs in one other important detail which is that here the longitudinal recirculating current flow centred on the non-uniform field region is confined to regions where the magnetic field is non-zero. Therefore, fully developed flows will not necessarily exist throughout the uniform field regions.

The analogous problem of a high-N flow proceeding from a straight duct into a diffuser when the field is uniform has been analysed by Walker, Ludford & Hunt (1971, 1972) but only for the idealized extreme cases of walls for which $\Phi = \infty$ and $\Phi = 0$ respectively. In the former case there is a constant potential difference between the (isolated) perfectly conducting walls, and the corresponding electric field can be either greater or less than the induced electric field at different places along the duct. Consequently there are, again, longitudinal recirculating currents but now over the whole length of the duct leading to both positive and negative pressure gradients. The behaviour of the flow depends on whether (i) only the non-conducting walls diverge or (ii) only the conducting walls diverge or (iii) both pairs of walls diverge In (i) a small velocity overshoot in the boundary layer of thickness $O(aM^{-\frac{1}{2}})$ ($2a$ being the separation of the non-conducting walls in the straight part of the duct) on the conducting wall reduces its displacement thickness to zero; the flow in (ii) is much

like that in a straight duct (Hunt & Stewartson 1965). Unlike (i) and (ii), the core current in (iii) has a component parallel to the conducting wall at the edge of the core. To reduce the associated tangential electric field to zero across the boundary layer requires a very large $O(M^{\frac{1}{2}}VB_0)$ induced electric field which implies the existence of $O(M^{\frac{1}{2}}V)$ velocities in that layer (and not necessarily in the streamwise direction!). When $\Phi = 0$ the behaviour of the flow is similar to that in case (iii) when $\Phi = \infty$ but currents and pressure gradients are lower by a factor of at least $O(M^{-\frac{1}{2}})$.

Experimental studies of such problems as these are infreqent in the MHD literature and, in fact, are difficult to realize in practice. Magnets have a finite length and if, as here, the length of the conducting walls of the duct exceeds the length of the magnet the flow will pass through non-uniform field regions upstream and downstream of the region of interest between them. The recirculating current flows at each non-uniform field region not only ensure that the potential difference between the conducting walls will be lower than expected but also promote distortions to the fully developed flow which can persist for substantial distances along the duct. In such cases the velocity distributions at the entry and exit parts of the duct are relatively unimportant since the electric currents there are flowing in regions where $\mathbf{B} = 0$ and their behaviour is governed solely by the potential distribution which satisfies Laplace's equation. On the other hand, if the duct lies wholly within the length of the magnet then the details of the inlet and outlet flows as well as their positions relative to the ends of the conducting walls become important. For any flow meeting a magnetic field the entry length (i.e. the length of duct required for the fully-developed flow to become established) is $O(1/N\Phi)$ when $N = O(1)$ and Φ is small (Shercliff 1962, § 3.3.2) and $O(a)$ when $N \gg 1$ and $\Phi = \infty$ (Walker *et al.* 1971) but the actual length will depend on the form of the flow. Here the flow entered the duct as a central jet with a mean velocity of about 50 V just upstream of the ends of the conducting walls. This suggests that the entry length would be longer than if, for example, a settling chamber and contraction had been inserted upstream of the conducting walls. In addition, the flow left the duct via similar pipework.

The analysis set out in § 2 presupposes that viscous and inertial effects are negligible, i.e. M, $N \gg 1$ and in the experiments described in § 3 these conditions are upheld over most of the flow. In § 2.2 the core flow solution of Walker *et al.* (1971) case (i) is generalized to include non-uniform fields and this is discussed in the light of recent work by Holroyd & Walker (1978) on the flow in non-conducting ducts. In particular, the first-order solution shows that velocity variations are confined to the plane of and determined by the magnetic field variations and that there are no longitudinal potential gradients and currents in the core. From this solution it is deduced that the usual condition for treating walls as perfect conductors, i.e. $\Phi \gg 1$ must be replaced by a stronger condition which is not satisfied by the present duct (and which, indeed, is virtually impossible to realize in practice). Once $\infty \gg \Phi > 0$ the general three-dimensional analysis becomes exceedingly complex and here further progress can only be made by neglecting the previously important but now insignificant variations in the plane of the magnetic field, even so, more simplifying assumptions are necessary to make the now two-dimensional analysis tractable. The solution presented in § 2.3 derives from the components of Ohm's law and therefore investigates the relationships between the current, potential and velocity distributions. Effectively the electric, or kinematic consequences of the flow are explored in marked contrast to the earlier

analysis for $\Phi = \infty$ when the current and potential distributions have no influence on the velocity distribution. Two independent approximations are employed which lead to almost identical answers. Moreover, the solutions are valid even when the field strength is small because it is unnecessary to invoke the inertialess and inviscid flow conditions.

The analyses show that an $O(aVB_0)$ potential difference along the duct is created by the longitudinal current flow(s) along the conducting walls and the presence of a significant midstream velocity component in a direction perpendicular to those walls is thereby implied. From measurements of the potential distribution between the conducting walls described in § 3 it is inferred that this predicted transverse flow exists and is significant. Also described in § 3 are measurements of distributions along the duct of pressure and potential difference between the conducting walls and they agree tolerably well with the predicted distributions over the whole length of the duct thereby underlining the relative unimportance of M and N.

Finally, in § 4 the successes and shortcomings of the work are discussed and its significance in relation to the current state of MHD duct flow research is examined.

2. Analysis

2.1. *Governing equations*

A dimensionless form of the equations and boundary conditions governing the steady motion of an isotropic electrically conducting liquid based on V the mean velocity of the flow at some point, a half the distance between the non-conducting walls, B_0 the value of the highest uniform magnetic field strength together with the fluid properties density ρ, conductivity σ, viscosity η and permeability μ was derived by Holroyd & Walker (1978). When the magnetic Reynolds number $R_m = \mu\sigma aV \ll 1$, the equations are

$$N^{-1}\mathbf{v}.\nabla\mathbf{v} = -\nabla h + \mathbf{j}\wedge\mathbf{B} + M^{-2}\nabla^2\mathbf{v}, \quad \mathbf{j} = -\nabla\phi + \mathbf{v}\wedge\mathbf{B} \tag{1a,b}$$

$$\nabla.\mathbf{v} = \nabla.\mathbf{j} = \nabla.\mathbf{B} = \nabla\wedge\mathbf{B} = 0, \tag{1c)–(f}$$

where $\mathbf{v}, h, \mathbf{j}, \phi$ and $\mathbf{B}\,[=(B_x(x,y), B_y(x,y), 0)]$ represent the non-dimensional variables velocity, pressure, electric current density, electric potential and magnetic flux density respectively and the co-ordinate axes are those defined in figures 1 and 2. $M = aB_0\sqrt{(\sigma/\eta)}$ is the Hartmann number and the interaction parameter $N = \sigma B_0^2 a/\rho V = M^2/R$ where $R = \rho Va/\eta$ is the Reynolds number of the flow. It will be assumed that the values of M and N are sufficiently large for viscous and inertial effects to be ignored except in extremely thin boundary layers on the walls and in regions where $\mathbf{B} \simeq 0$ so that (1a) reduces to

$$\nabla h = \mathbf{j}\wedge\mathbf{B}. \tag{1g}$$

The conductance ratio $\Phi = \sigma_w t/\sigma a$ where σ_w and t represent the conductivity and thickness of the conducting walls.

2.2. *Analysis of the flow when* $\Phi = \infty$ (*perfectly conducting walls*)

Following the method of analysis employed by Walker *et al.* (1971) the flow will be assumed to have the usual régimes typical of high-M flows, namely Hartmann layers of thickness $O(M^{-1})$ on the non-conducting walls, boundary layers of thickness

$O(M^{-\frac{1}{2}})$ on the conducting walls and a central inviscid core flow where the variables may be expressed as power series in $M^{-\frac{1}{2}}$, e.g. $\mathbf{v} = \mathbf{v}^{(0)} + M^{-\frac{1}{2}}\mathbf{v}^{(\frac{1}{2})} + \ldots$.

The two-dimensional form of the imposed magnetic field allows it to be defined in terms of $A(x, y)$, the single z component of a magnetic vector potential, and $\Psi(x, y)$, a magnetic scalar potential, i.e. $\mathbf{B} = \nabla \wedge (0, 0, A) = \nabla\Phi$. Curves defined by A = constant are magnetic field lines which together with curves Ψ = constant form a two-dimensional orthogonal curvilinear co-ordinate system.

In terms of this co-ordinate system $(1q)$ may be written as

$$(B\partial h^{(0)}/\partial A, B\partial h^{(0)}/\partial\Psi, \partial h^{(0)}/\partial z) = (j_z^{(0)} B, 0, -j_A^{(0)} B).$$

The second component of this shows that $h^{(0)} = h^{(0)}(A, z)$, i.e. the pressure is constant along a field line, while the other components relate the current density components $j_A^{(0)}$ and $j_z^{(0)}$ to the field strength and partial differentials of $h^{(0)}$. Using these latter expressions in conjunction with $(1d)$ enables an expression for $j_\Psi^{(0)}$ to be found so that the three current density components may be written as

$$j_A^{(0)} = -\frac{1}{B}\frac{\partial h^{(0)}}{\partial z}, \quad j_\Psi^{(0)} = B\frac{\partial h^{(0)}}{\partial z}\int_0^\Psi \frac{\partial B^{-2}}{\partial A}d\Psi', \quad j_z^{(0)} = \frac{\partial h^{(0)}}{\partial A}; \qquad (2a, b, c)$$

(2*b*) is, in fact, a simpler form of a general expression deduced by Kulikovskii (1968, equation (1.8)). At a non-conducting wall, defined as

$$\Psi = F(A, z), \quad j_n^{(0)} = \operatorname{sgn}(\hat{\mathbf{n}} \cdot \mathbf{B})\, M^{-1}(\nabla \wedge \mathbf{v}^{(0)})$$

(where $\hat{\mathbf{n}}$ is the unit normal to the wall directed into the fluid) provided there is a significant component of $\mathbf{B}$ normal to the wall, i.e. $\hat{\mathbf{n}} \cdot \mathbf{B} = O(1)$ (Hunt & Ludford 1968). Here this may be written as

$$-j_A^{(0)}\frac{\partial F}{\partial A} + j_\Psi^{(0)} - \frac{1}{B}j_z^{(0)}\frac{\partial F}{\partial z} = 0. \qquad (3)$$

If the flow is confined between non-conducting walls denoted as F_1 and F_2 then by combining (2) and (3) it may be shown that

$$\partial\left(h^{(0)}, \int_{F_1}^{F_2} B^{-2}d\Psi\right)\Big/\partial(A, z) = 0$$

so that

$$h^{(0)} = h^{(0)}\left(\int_{F_1}^{F_2} B^{-2}d\Psi\right)$$

which implies that the core currents flow on surfaces defined by

$$\int_{F_1}^{F_2} B^{-2}d\Psi = \text{constant}.$$

(Note that in Holroyd & Walker (1978, §, 3.1) physical arguments are used to show that this result is true for a three-dimensional non-uniform case provided $|\mathbf{j}| \ll |\mathbf{v}|$.) In the present case F_1 and F_2 define two parallel planes and so the z dependence is lost. Consequently the current flow will be across the duct in the z direction since $\partial h^{(0)}/\partial z = 0$ and therefore $j_A^{(0)} = j_\Psi^{(0)} = 0$. Furthermore, $j_z^{(0)} = dh^{(0)}/dA$ is constant along a field line.

The absence of core currents at the edge of the core parallel to the conducting walls eliminates the possibility of a longitudinal electric field component there. This is

important because without such a field there can be no large field *normal* to the conducting wall and hence no high velocity flow in the boundary layer there. From (1*b*) $\partial\phi^{(0)}/\partial\psi = 0$ so that $\phi^{(0)} = \phi^{(0)}(A, z)$ and, in line with the above arguments, satisfies $\phi^{(0)}(A, z = \pm\lambda) = \pm$ constant at the perfectly conducting walls. For consistency with the uniform field case where $\phi \propto z$ (Hunt & Stewartson 1965) and $A = -B_y x$, it is sufficient to take $\phi^{(0)} = z\Delta\phi/2\lambda$ where $\Delta\phi$ is the potential difference between the conducting walls.

Since $\phi^{(0)}$ is independent of A it follows from (1*b*) that $v_z^{(0)} = \partial\phi^{(0)}/\partial A = 0$. The two remaining non-zero velocity components may now be derived from a stream function $\Theta(x, y)$ as $\mathbf{v}^{(0)} = \nabla \wedge (0, 0, \Theta)$ in which case the flow rate along the duct at any point is given by

$$\int_2^1 \int_{-\lambda}^{\lambda} v_x^{(0)}\, dy\, dz = 2\lambda \int_2^1 \frac{\partial\Theta}{dy}\partial y = 2\lambda\{\Theta(F_1) - \Theta(F_2)\} = 4\lambda, \tag{4}$$

while at the edge of the core adjacent to the non-conducting walls

$$\Theta(F_1), \quad \Theta(F_2) = \text{constant} \tag{5}$$

since $\mathbf{v}^{(0)} \cdot \hat{\mathbf{n}} = 0$ there. The only non-zero component of (1*b*) can now be written as

$$j_z^{(0)} = -\frac{\Delta\phi^{(0)}}{2\lambda} + B\frac{\partial\Theta}{\partial s}, \tag{6}$$

where s is the distance measured along a field line (so that $\delta\psi = B\delta s$). By integrating (6) along a field line and using (4) and (5) it may be shown that

$$\Theta = 2\int_0^S \frac{ds}{B} \Big/ \int_0^{S_0} \frac{ds}{B}, \tag{7}$$

where S_0 is the total length of a field line between the non-conducting walls. Equation (7) shows that Θ, and hence the velocity distribution, is completely determined by the magnetic field only and in particular by integrals along field lines of the form $\int B^{-1} ds$. Holroyd & Walker (1978) showed that in variable-area non-conducting ducts the flow follows equipotential surfaces defined by $\int_0^{S_0} B^{-1} ds =$ constant but clearly this is not the case here even though the flow is confined between non-conducting walls. This apparent inconsistency stems from the different magnitudes of the current flow in the two cases; here $\mathbf{j}$, $\mathbf{v}$ and ϕ are all $O(1)$ while in Holroyd & Walker's case $\mathbf{j} = O(M^{-\frac{1}{2}})$ while $\mathbf{v}$ and ϕ were $O(1)$. Consequently different solutions arise in the two cases. On the other hand, if the perfectly conducting walls were replaced by insulating walls then $\mathbf{j}$ would be $O(M^{-\frac{1}{2}})$ but the equipotential surfaces could not be defined because S_0 and $\mathbf{B}$ are independent of z. In such cases the only possible core flow is $\mathbf{v} = O(M^{-\frac{1}{2}})$ at most which implies that the flow is carried in the boundary layer on the walls parallel to $\mathbf{B}$ (see, for example, Walker *et al.* 1972).

If a three-dimensional non-uniform field is considered (rather than the present two-dimensional one) then the conducting walls would not necessarily be parallel to the field lines everywhere. In such cases there would be a radically different internal flow structure comprising several distinct core flow regions separated by shear layers of thickness $O(M^{-\frac{1}{2}})$ centred on those field lines passing through the corners of the duct (Hunt & Shercliff 1971). It should also be borne in mind that if the non-conducting

walls are parallel but not at right angles to the field lines then another solution may have to be sought as in the equivalent uniform field case (Shercliff 1975).

Ludford & Walker (1980) have derived the two partial-differential equations governing the flow in the boundary layers on the conducting walls but solutions, which depend on the form of the magnetic field, have not been sought. However, if $\mathbf{B} = (0, 1, 0)$ they reduce to the governing equations for the corresponding boundary layer in the uniform field case (Walker *et al.* 1971) which suggests that there will be no major differences between the flows in the two cases.

The potential difference between the conducting walls may be found by integrating (1*b*) over their area A_0, i.e.

$$\Delta\phi^{(0)} = \frac{2\lambda}{A_0}\left\{-\iint_{A_0} j_z^{(0)}\,dx\,dy + \iint_{A_0} B\frac{\partial\Theta}{\partial s}\,dx\,dy\right\}. \tag{8}$$

The first integral on the right-hand side represents the net current flow between the conducting walls and its value depends on the electrical connexion between them; if they are electrically isolated from each other its value is zero. The second integral can be evaluated by using (7). However, the value of $\Delta\phi$ given by (8) can only be approximately true for several reasons. If $\mathbf{B} \neq 0$ near the ends of the conducting walls then the flows of current and fluid there, as well as in regions where $\mathbf{B}$ is so small that the conditions $M, N \gg 1$ are not satisfied, will not be given by (6) and (7) but will undoubtedly have a complex three-dimensional form. However, where $\mathbf{B} = 0$ the first integral in (8) will still be valid (if evaluated at $z = \pm\lambda$) while the second will be zero.

When the conducting walls are electrically isolated from each other systems of recirculating currents on surfaces perpendicular both to these walls and the field lines are set up. Where $\Delta\phi/2\lambda < v_x B_y$ (i.e. regions of maximum velocity and flux density) $j_z^{(0)}$ will flow so as to induce a braking force on the flow; this effect is reversed where $\Delta\phi/2\lambda > v_x B_y$. Between such regions the conducting walls act as short circuits for the current. When the currents flow in regions where $\mathbf{B} = 0$ the fluid acts as a short circuit but does not feel any electromagnetic force.

So far the term 'perfectly-conducting wall' has been loosely defined as a wall for which $\Phi \gg 1$. A more precise definition may be derived from the fact that the potential drop, $a\,VB_0\delta\phi$, *along* these walls due to the longitudinal current flow in them should be very small; in non-dimensional terms $\delta\phi \ll 1$. Here, a typical length scale for the recirculating currents is the length of the duct L and so it follows from (1*b*) and (1*d*) that

$$\delta\phi \approx (\sigma/\sigma_w)\{(L/a)j_z^{(0)}/(t/a)\} = L^2(\sigma/\sigma_w)/at$$

(since $j_z^{(0)} = O(1)$). Therefore, if $\delta\phi \ll 1$

$$\sigma_w at/\sigma L^2 = \Phi a^2/L^2 = (\sigma_w t/L)/(\sigma L/a) \gg 1$$

and this may be interpreted as (conductance *along* duct walls)/(conductance *across* duct in fluid) $\gg 1$. Clearly this is a much stricter condition than $\Phi \gg 1$ and is difficult, if not impossible, to realize in practice. Since the present duct does not satisfy this condition, the flow in it must be re-analysed to take into account the finite conductivity of its conducting walls.

2.3. *Analysis of the flow when the conducting walls have finite conductivity*

Although a general three-dimensional analysis of this problem is complex it is possible to predict some of the integral features of the flow in a relatively straightforward manner by making several simplifying assumptions. The flow may reasonably be expected to become more like that in a non-conducting rectangular duct (see Walker *et al.* 1972); Kit *et al.* (1970) as Φ decreases. Here, since the walls are still highly conducting, it is probable that core velocity gradients will remain $O(1)$ while $v_y \ll v_x, v_z$ (when $\Phi = \infty$ it can be deduced from (7) that $|v_y| < 0{\cdot}035$ for the field used in the following experiments). At the non-conducting walls the relevant boundary condition implies that $j_y \ll j_x, j_z$. The three components of (1*b*) now reduce to

$$j_x = -\partial\phi/\partial x - v_z B_y, \quad 0 = -\partial\phi/\partial y + v_z B_x, \quad j_z = -\partial\phi/\partial z + v_x B_y. \quad (9a,b,c)$$

To further simplify matters it will be assumed that there is still no $O(1)$ change in ϕ across the boundary layers on the conducting walls and that, as in Shercliff's low-N analysis, B_x can be neglected. In addition, by inspecting the components of the field used here shown in figure 2 (plotted, for convenience, as $2\lambda B_y$ and $2\lambda B_x$) it can be seen that variations of B_y with y are unimportant, i.e. $B_y = B_y(x)$. In marked contrast with the analysis for perfectly conducting walls where the problem was reduced to two-dimensions in the Oxy plane, here all dependence of y has been eliminated leaving the problem two-dimensional in the Oxz plane.

Further progress can be made in two ways by making different approximations.

Analysis (i). Let $j_x = 0$ so that $j_z = j_z(x)$ and take the conducting walls to have equal non-dimensional thickness $t' \ll 1$ thereby allowing the 'thin-walled' boundary condition to be applied [see Holroyd & Walker 1978, equation (2.4*c*)]. Here it may be written as

$$j_z = -\Phi\partial^2(\tfrac{1}{2}\Delta\phi)/\partial x^2. \quad (10)$$

Integrating (9*c*) over the cross-section of the duct yields

$$4\lambda j_z(x) = -2\Delta\phi(x) + 4\lambda B_y(x). \quad (11)$$

Combining (10) and (11) gives a governing equation for $\Delta\phi(x)$, namely

$$\left(\frac{\partial^2}{\partial x^2} - \frac{1}{\lambda\Phi}\right)\Delta\phi = -\frac{2}{\Phi}B_y(x), \quad (12)$$

whose solution is completed by two boundary conditions which are that the longitudinal current flow in the conducting walls which is proportional to $\partial(\Delta\phi)/\partial x$ is zero at each end of those walls.

Note that the solution to (12) does not show how ϕ varies between the conducting walls while $\Delta\phi$ itself is independent of the velocity distribution.

Analysis (ii). Let $v_z = 0$ so that $v_x = 1$ and approximate the form of $B_y(x)$ by step functions. In each range of x for which $B_y =$ constant the equations governing the potential distribution in the fluid (ϕ) and walls (ϕ_{w+} at $z = \lambda$ and ϕ_{w-} at $z = -\lambda$) may be derived by differentiating (9*a* and 9*c*) with respect to x and z respectively, adding them and using (1*d*) to give

$$\left(\frac{\partial^2}{\partial x^2} + \frac{\partial^2}{\partial z^2}\right)(\phi_f - zB_y) = 0, \quad (13a)$$

$$\left(\frac{\partial^2}{\partial x^2} + \frac{\partial^2}{\partial z^2}\right)\phi_w = 0. \quad (13b)$$

In either conducting wall $j_{zw} = -\sigma' \partial\phi_w/\partial z$ where $\sigma' = \sigma_w/\sigma$ and in the fluid

$$j_z = -\partial(\phi_f - zB_y)/\partial z.$$

At $z = \pm\lambda$ the expressions for ϕ_f, ϕ_w and j_z, j_{zw} may be equated (Shercliff 1965, § 5.8, 5.9) while since no current leaves or enters the duct at the outer faces of the conducting walls then $j_{zw} = 0$ at $z = \lambda + t_1'$ and $-\lambda - t_2'$ (t_1' and t_2' are the non-dimensional thickness of these walls). The solution to (13) satisfying these conditions is

$$\phi(x,z) = B_y f(z) + \phi_{w+}(x, \lambda + t_1' > z > \lambda) + \phi_f(x, \lambda > |z|) + \phi_{w-}(x, -\lambda > z > -\lambda - t_2'), \quad (14a)$$

where

$$f(z) = \begin{cases} \lambda & \text{for} \quad z > \lambda, \\ z & \text{for} \quad \lambda > |z|, \\ -\lambda & \text{for} \quad z < -\lambda, \end{cases} \quad (14b)$$

and

$$\phi_{w+} = \Sigma \frac{\cos k(\lambda + t_1' - z)}{\sin k\lambda \cos kt_1' + \sigma' \cos k\lambda \sin kt_1'} (P_k \sinh kx + Q_k \cosh kx), \quad (14c)$$

$$\phi_f = \Sigma (\sin kz + R_k \cos kz)(P_k \sinh kx + Q_k \cosh kx), \quad (14d)$$

$$\phi_{w-} = \Sigma \frac{\cos k(\lambda + t_2' + z)}{\sin k\lambda \cos kt_2' + \rho' \cos k\lambda \sin kt_2'} (P_x \sinh kx + Q_k \cosh kx), \quad (14e)$$

and are zero *outside* the ranges of z indicated in (14a).

$$R_k = \frac{\cos k\lambda \cos kt_1' - \sigma' \sin k\lambda \sin kt_1'}{\sin k\lambda \cos kt_1' + \sigma' \cos k\lambda \sin kt_1'} = -\frac{\cos k\lambda \cos kt_2' - \sigma' \sin k\lambda \sin kt_2'}{\sin k\lambda \cos kt_2' + \sigma' \cos k\lambda \sin kt_2'}$$

which can only be true if

$$\tan 2k\lambda = \sigma'(\tan kt_1' + \tan kt_2')/(\sigma'^2 \tan kt_1' \tan kt_2' - 1). \quad (15)$$

The summations in (14c, d, e) include all the positive eigenvalues, k, of (15).

There are different values of P_k and Q_k for every range of x over which B_y = constant. At a station where there is discontinuous change in $B_y(x)$, say at $x = b$, the values of P_k and Q_k for $x < b$ and $x > b$ for each value of k are related to each other through two equations expressing continuity at $x = b$ for all z of j_x (proportional to $\partial\phi/\partial x$) and $\partial\phi/\partial z$. These are

$$(P_k^+ - P_k^-)\cosh kb + (Q_k^+ - Q_k^-)\sinh kb = 0 \quad (16a)$$

and

$$(P_k^+ - P_k^-)\sinh kb + (Q_k^+ - Q_k^-)\cosh kb = -2(B_y^+ - B_y^-)\sin k\lambda/k^2 F_k, \quad (16b)$$

where

$$F_k = \frac{\sigma'(kt_1' - \sin kt_1' \cos kt_1')}{2k(\sin k\lambda \cos kt_1' + \sigma' \cos k\lambda \sin kt_1')^2} + \lambda(1 + R_k^2) + \frac{1}{2k}(1 - R_k^2)\sin 2k\lambda + \frac{\sigma'(kt_2' - \sin kt_2' \cos kt_2')}{2k\{\sin k\lambda \cos kt_2' + \sigma' \cos k\lambda \sin kt_2'\}^2} \quad (17)$$

and the superscripts + and − indicate values for $x > b$ and $x < b$. The reasons for using continuity of $\partial\phi/\partial z$ rather than ϕ and the derivation of (17) are given in the appendix. If there are n discontinuous changes in $B_y(x)$ along the duct then for each value of k there will be n pairs of the equations (16) but $(n+1)$ each of the unknowns P_k and Q_k. The two extra equations required to complete the solution follow from the condition that $j_x = 0$ and hence $P_k \cosh kx + Q_k \sinh kx = 0$ at each end of the duct.

It may be shown that when $t_1' = t_2' = t'$ and $kt' \ll 1$ then the transcendental equation (15) and the complete solution reduces to that obtained by Vasil'ev & Lavret'ev (1969).

Comparison of solutions from analyses (i) *and* (ii)

For this purpose the magnetic field described in figure 2 may be represented simply as $B_y(x) = s(x-14{\cdot}4) - \frac{1}{2}s(x+0{\cdot}6) - \frac{1}{2}s(x-17{\cdot}6)$ where $s(\xi) = 1$ for $\xi > 0$ and is zero otherwise. Let the ends of the conducting walls be at $x = 21{\cdot}8$ and $x = -19{\cdot}6$. The relevant non-dimensional parameters of the present duct are $\lambda = 1{\cdot}256$, $t_1' = 0{\cdot}183 = t_2'/1{\cdot}5$ and $\sigma' = 56{\cdot}8$ and in analysis (i) $t' = \frac{1}{2}(t_1' + t_2')$ so that $\Phi = \sigma' t'$.

Calculations of $\Delta\phi$, the potential difference between the conducting walls, by the two analyses differ by no more than $0{\cdot}15\,\%$ of their mean value anywhere along the duct while analysis (ii) indicates that the potential difference between the inner and outer faces of either conducting wall is less than $0{\cdot}0015\Delta\phi$. An even more significant result is obtained by comparing the potential distribution across the duct, $\phi(z)$ calculated from analysis (ii) with an assumed linear distribution calculated from analysis (i), namely $z\Delta\phi/2\lambda$ (which corresponds to a uniform velocity profile $v_x(z) = 1$). For any position along the duct

$$\text{maximum value of } |\phi(z) - z\Delta\phi/2\lambda| \leqslant 0{\cdot}0075\Delta\phi$$

and this has two important implications, namely (i) j_x in the fluid has negligible effect on the potential distribution and so (ii) if the slope $\partial\phi/\partial z$ of a measured potential distribution varies with z then the variation can be attributed to a non-uniform velocity profile in accordance with (9*c*).

These arguments show that results derived from analysis (i) are quite satisfactory for this work. At smaller values of σ', analysis (ii) would be more useful.

3. Experimental work

3.1. *Apparatus*

Experiments using mercury flowing along the duct shown in figure 1 situated in the field whose principal components are plotted, for convenience, as $2\lambda B_x^*/B_0$ and $2\lambda B_y^*/B_0$, ($B_z = 0$) in figure 2 were carried out to satisfy two objectives, namely (i) to verify the theoretical predictions of the potential difference between the conducting walls and the pressure distribution along the duct and (ii) to elucidate the internal structure of the flow by measurement of the potential distribution inside the duct. (Unfortunately, lack of time in an experimental programme of which these experiments were a minor part precluded the use of hot film probes to measure velocity distributions.)

The electromagnet, flow circuit, manometer system, probe for measuring potential distributions inside the duct and trolley for supporting the duct and allowing it to be moved longitudinally relative to the magnet are described in Holroyd (1976, 1979).

Basic details of the duct are shown in figure 1. Of the 1·44 m ($= 41{\cdot}41a$) long copper walls, one was 6·35 mm thick and the other 9·525 mm in order to accommodate the bolts needed to affix the 15 pressure taps along its length. Although this apparently destroyed the symmetry of the duct the analysis and results showed that it was not significant. These walls were held 87·3 mm ($= 1{\cdot}256 \times 2a$) apart by PVC (non-conducting)

walls and clamped together by 42 stainless-steel bolts passing through the PVC walls. A neoprene gasket at the PVC/copper wall junctions prevented leaks and the copper walls were electrically isolated from each other by insulating the bolts from one wall by nylon bushes (see corner detail in figure 1). About two-thirds of the way along the duct (from the flow inlet) provision was made for inserting a probe into the flow. A circular copper disk fitted into a mating hole in the thicker copper wall, the seal being effected by an O-ring, and the probe stem passed through it at a point near its periphery. By rotating the disk the axis of the probe could be moved from near one PVC wall to half-way between them. Motion of the probe at right angles to the conducting walls (i.e. parallel to the z axis) was achieved by a simple nut and screw traversing gear mounted on the disk.

The general form of the magnetic field is shown in figure 2. Over most of the first 450 mm ($=12{\cdot}95a$) of the magnet the flux density, $B_y^* = B_0$, was uniform with a maximum value of $0{\cdot}56T$ while over the remaining 556 mm ($=16a$) $B_y^* = \frac{1}{2}B_0$. Thus the maximum Hartmann number was 505. At the highest flow rate the Reynolds number was 7500.

3.2. *Variation of the potential difference between the conducting walls, $\Delta\phi^*$*

In figure 2 are shown measurements of $\Delta\phi^*$ along the duct plotted as $\Delta\phi = \Delta\phi^*/aVB_0$ for three different positions of the duct relative to the magnetic field to see how this affected the $\Delta\phi$ distribution and hence the current flow along and across the duct and hence (§ 3.4) the pressure distribution. Two extreme positions left a large portion of the duct either upstream or downstream of the magnet so that the flow there was not subjected to the influence of electromagnetic forces since $\mathbf{B} \equiv 0$; the third position was approximately midway between the others. Also shown in figure 2 are (i) the appropriate theoretical distributions derived from (12) with $B_y(x)$ given by the measured values of B_y^* on the centre-line of the air gap of the magnet and an assumed linear variation between adjacent points and (ii) the distribution of $2\lambda B_y$ which is numerically equal to $2\lambda \times$ mean value of induced electric field.

It can be seen from figure 2 that there is close agreement between the measured and predicted distributions. The obvious discrepancies occur in the high field strength region where the experimental values are 5 % lower than expected but there are fractional differences of similar magnitude but opposite sign near the ends of the duct when they are remote from the magnet. These errors are probably due to the longitudinal recirculating current flows which were neglected in analysis (i). For example, from the mid-section of the high field strength region there will be current flows, j_x, both upstream and downstream due to the potential gradients in the core. These currents will tend to augment the current flow, j_z, by an amount say, Δj_z, near $z = 0$. To satisfy continuity (1*d*) $\Delta j_z \simeq \partial j_x/\partial x$ while from (1*b*) it follows that

$$\partial j_x/\partial x = -\partial^2\phi/\partial x^2 - \partial(v_z B_y)/\partial x.$$

From these two relationships and (10) it follows that $\Delta j_z \simeq j_z/\Phi - \partial(v_z B_y)/\partial x$. Therefore, the magnitude of the term $4\lambda j_z$ in (11) could be increased by a factor of $(1 + \Phi^{-1})$ and it follows from that same equation that $\Delta\phi$ will be increased or decreased by the same factor depending upon whether j_z is greater or less than zero. Since $\Phi \simeq 13$ here such errors in $\Delta\phi$ are consistent with the observed fractional discrepancies over $-13 < x < 0$ where $j_z > 0$ and $-34 < x < -13$ and $17 < x < 28$ where $j_z < 0$. So far

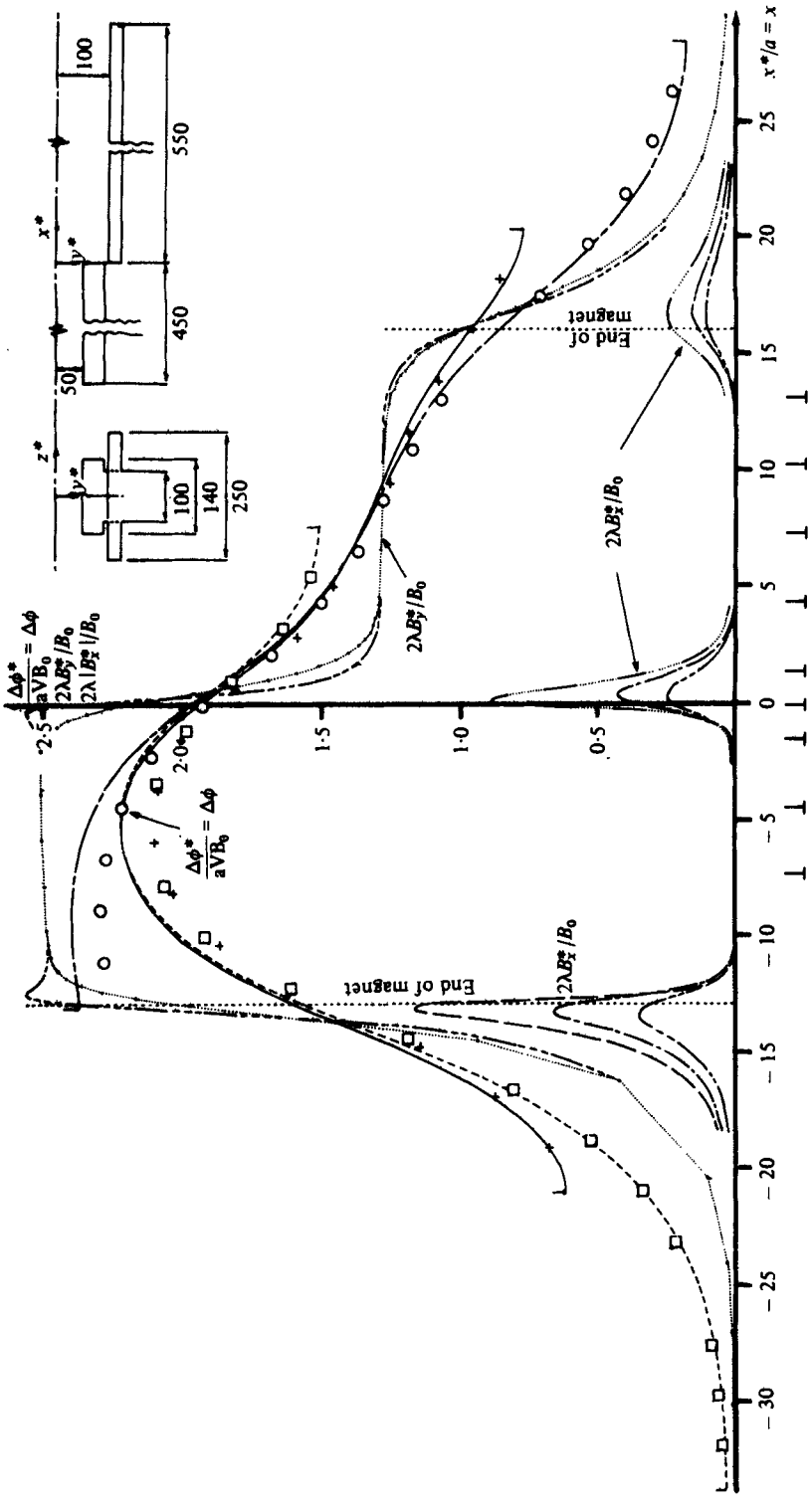

FIGURE 2. Predicted (curves) and measured (points) distributions along a duct of potential difference between conducting walls, $\Delta\phi^*$. The short vertical lines on the ends of the curves indicate the ends of the conducting walls. Principal components of magnetic field are plotted as $2\lambda B_y/B_0$ and $2\lambda|B_x|/B_0$ ($B_z^* \equiv 0$); values are measured at $z = 0$ for specific values of y. The larger dots on the distribution of B_y^* ($y = 0$) indicate measured values; linear variation indicated between neighbouring values was used in solution of (12). ⊥ indicates the positions where the distributions in figure 3 were recorded. Potential distributions, (M, N, R): ○—·—○, (494, 34·54, 7053); +——+, (506, 35·84, 7142); □– – –□, (506, 35·84, 7142). Components of magnetic field: ·····, $2\lambda B_y^*/B_0$, $y = 0$; – – – –, $2\lambda B_y^*/B_0$, $y = 0{\cdot}699$; —·—·—, $2\lambda B_x^*/B_0$, $y = 0{\cdot}476$; —·—·—, $2\lambda B_x^*/B_0$, $y = 0{\cdot}748$; —·····—, $2\lambda B_x^*/B_0$, $y = 1{\cdot}042$; ——, $2\lambda B_x^*/B_0$, $y = 1{\cdot}122$. At the top right-hand corner are shown half-plan and end elevation views of the pole pieces of the magnet with leading dimensions in mm.

the term $\partial(v_z B_y)/\partial x$ has not been considered; the results of Shercliff (1962) and Kit *et al.* (1970) suggest that it will only be important where B_y is varying. Its magnitude can be estimated as $\partial^2(\Delta\phi)/\partial x^2$ in such regions and here an upper limit of about 0·05 can be deduced from the distributions in figure 2. Consequently it does not significantly affect the argument.

To see how $\Delta\phi^*$ varied with M and N its value was recorded at $x^*/a = -5{\cdot}89$ with the duct in the central of the three positions described above for various field strengths and flow rates. At this position the current flow along the walls is zero since

$$\partial(\Delta\phi)/\partial x = 0.$$

Plots of $\Delta\phi^*$ against mean velocity V were linear with slopes proportional to B_0 (within experimental error) but after extrapolation to $V = 0$ the value of $\Delta\phi^*$ was not zero but differed by no more than 27μV ($= 0{\cdot}3\,\%$ of the maximum measured value of $\Delta\phi^*$). It is quite possible that this offset was due to the thermal e.m.f. created at the mercury–copper interfaces. During a 2 h experiment both the mercury and air temperatures could rise, typical values being 8 and 3 K respectively. Therefore, the temperatures of the mercury and copper were not necessarily identical – a difference of 2 K would account for the aforementioned offset in $\Delta\phi^*$ (see Kaye & Laby 1973, § 1.5). In this experiment

$$\Delta\phi = \Delta\phi^*/aVB_0 = 2{\cdot}093 \text{ for } 90 < M < 505 \text{ and } 1{\cdot}5 < N < 3500.$$

3.3. *Potential distributions across the duct in the fluid*

These distributions were made by traversing the potential probe over the centre-plane $y = 0$ of the duct. The design of the probe limited the z-wise range of motion to about 60 % of the duct width from the thinner of the conducting walls while the design of the duct limited the position of the probe tip to 0·926 m $= 26{\cdot}65a$ from the upstream end of the conducting walls. This latter fact implies that measurements from a traverse relate to that position of the duct relative to the magnetic field and no other – results from a traverse with the probe tip displaced a distance x' nearer to the upstream end of the duct and the duct moved an equal distance downstream would not necessarily be the same. However, from figure 2 it can be seen that provided there is no excessive length of duct upstream or downstream of the magnet then over the central 75 % or so of the magnetic field $\Delta\phi$ is fairly insensitive to the actual position of the duct. This suggests that the potential distribution in the fluid might be so too.

Distributions of the potential ϕ^* at nine different positions with respect to the magnetic field in the range $-7{\cdot}3 < x^*/a < 13{\cdot}2$ (x^* = position of probe tip) are summarized in figure 3. The data is plotted as $\phi = \phi^*/aVB_0$ and for each set of results a straight line indicates the theoretical distribution of ϕ for a uniform velocity profile while the value quoted at the wall is $\frac{1}{2}\Delta\phi$. Clearly, though, the measured distributions are nonlinear; at $x^*/a = -7{\cdot}28$ the potential gradient $\partial\phi/\partial z$ near the centre of the duct is less than the indicated linear distribution but as the conducting wall is approached this situation is reversed. Now, if, as was proposed in § 2, $\partial\phi/\partial z$ represents the velocity profile $v_x(z)$ to a good approximation, then at $x^*/a = -7{\cdot}28$ the velocity near the wall is about three times larger than that at the centre of the duct. On moving downstream to $x^*/a = -1{\cdot}44$ a nearly uniform velocity profile may be inferred from the results but just a little further downstream at $x^*/a = 0$ large velocities near the

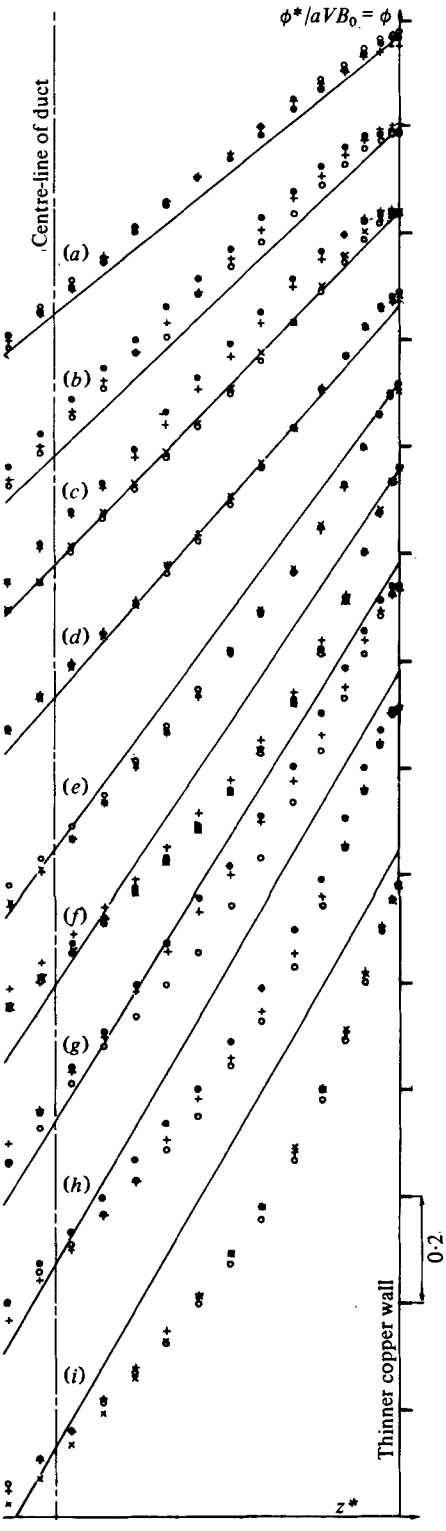

FIGURE 3. Distribution of potential ϕ^* on plane $y = 0$ at the positions x^*/a indicated by $\perp$ on figure 2 (x^* is the position of the probe tip). The ends of the conducting walls are at $x^*/a + 14{\cdot}78$ and $x^*/a - 26{\cdot}63$. (*a*) $x^*/a = 13{\cdot}17$, $\frac{1}{2}\Delta\phi = 0{\cdot}515$, ($M$, N, R): ○, (513, 131·4, 2006); ●, (505·5, 114·3, 2236); +, (44·9, 90·3, 2234). (*b*) $x^*/a = 10{\cdot}27$, $\frac{1}{2}\Delta\phi = 0{\cdot}612$, ($M$, N, R): ●, (474, 118·1, 1901); ○, (475, 83·9, 2684); +, (512, 97·8, 2680). (*c*) $x^*/a = 7{\cdot}35$, $\frac{1}{2}\Delta\phi = 0{\cdot}662$, ($M$, N, R): ●, (478, 120·3, 1902); +, (438, 101·1, 1901); ×, (436, 71·9, 2644); ○, (437, 52·1, 3670). (*d*) $x^*/a = 4{\cdot}39$, $\frac{1}{2}\Delta\phi = 0{\cdot}731$, ($M$, N, R): +, (490, 76·9, 3020); ×, (417·5, 57·7, 3020); ○, (417·5, 47·6, 3663). (*e*) $x^*/a = 1{\cdot}45$, $\frac{1}{2}\Delta\phi = 0{\cdot}875$, ($M$, N, R): +, (490, 112·6, 2134); ○, (490, 79·5, 3023); ×, (447, 93·3, 2138). (*f*) $x^*/a = 0$, $\frac{1}{2}\Delta\phi = 0{\cdot}969$, ($M$, N, R): +, (506, 144·6, 1769); ●, (506, 117·9, 2169); ×, (506, 99·3, 2576); ○, (506, 84·6, 3025). (*g*) $x^*/a = -1{\cdot}44$, $\frac{1}{2}\Delta\phi = 1{\cdot}047$, ($M$, N, R): ●, 477, 102·2, 2230); +, (396, 70·6, 2227); ○, (307, 35·2, 2675). (*h*) $x^*/a = -4{\cdot}37$, $\frac{1}{2}\Delta\phi = 1{\cdot}120$, ($M$, N, R): ●, (478, 102·2, 2234); +, (478, 67·1, 3406); ○, (572, 76·9, 3415). (*i*) $x^*/a = -7{\cdot}28$, $\frac{1}{2}\Delta\phi = 1{\cdot}052$, ($M$, N, R): ○, (489, 106·8, 2240); +, (443. 87·6, 2240); ×, (443, 58·25, 3368).

conducting walls are again indicated. At $x^*/a = 4{\cdot}39$ the velocity profile again appears to be uniform and remains so for the other readings.

The complementary function part of the solution to (12) suggests that the current flows in the conducting walls due to a sudden change in field strength near $x = x_0$ decay as $\exp\{-x'/(\lambda\Phi)^{\frac{1}{2}}\} \approx \exp(-\frac{1}{4}x')$ here where $x' = x - x_0$. If it is assumed that the inferred non-uniform velocity profile there decays to its appropriate fully-developed flow form in the same manner then it may be deduced from the above results for $x/a^* < 0$ that where the flow first meets the magnetic field the velocity near a conducting wall (i.e. near $z^* = \lambda a$) could be larger than that at $z^* = 0$ by a factor of about 20 ($= O(M^{\frac{1}{2}})$ here!). By the time the flow reaches the next change in field strength the velocity profile is nearly uniform but it is then similarly distorted again, although to a lesser extent, before finally becoming uniform after a shorter distance.

Such velocity profiles are most unlike those predicted for a duct with perfectly conducting walls. In fact, the behaviour of the flow is more like that found by Kit *et al.* (1970) in an insulating rectangular duct at low values of N and predicted by Shercliff (1962, § 3.3.3), again for low values of N, for ducts whose conducting walls have low values of Φ, but here the differences in velocity across the duct are far greater. They also persist for a distance of $14a$ which is much greater than the $aR/\Phi M^2$ predicted by Shercliff (1962, § 3.3.2; low N and Φ) and the aN predicted by Walker *et al.* (1971; $N \gg 1$, $\Phi = \infty$).

Another feature of the potential distributions shown in figure 3 is that they vary with M and N. Although the amount of data does not allow any definite conclusions to be reached, it would appear that for a given value of M the non-uniform velocity profiles persist over longer distances for smaller values of N (and hence larger values of R). In some cases, particularly at $x^*/a = 7{\cdot}35$ and $x^*/a = 9{\cdot}68$ there is evidence of a non-symmetric potential distribution about the centre of the duct as M and N vary which presumably is related to the non-symmetry of the duct.

3.4. *Pressure distributions along the duct*

Distributions of the pressure p along the duct measured at the mid-point of the thicker conducting wall, i.e. $y = 0$, $z = -\lambda$, are plotted in terms of

$$h = p/\rho V^2 N = p/\sigma a V B_0^2$$

in figure 4 for three different positions of the duct relative to the magnetic field similar to those employed when measuring $\Delta\phi^*$ (see § 3.2). In each case the corresponding theoretical distribution was deduced from (1g) as $h = \text{constant} - \int_0^x j_z B_y \, dx'$ with j_z given by (11) and the solution to (12). To obtain the value of the constant of integration a tracing of the theoretical curve was superposed on a plot of the experimental points and their relative positions varied until optimum agreement was observed. The middle theoretical distribution in figure 4 serves for two sets of results with the duct in slightly different positions except over short lengths near where the flow enters and leaves the duct.

The shapes of these distributions are readily inferred from distributions of $\Delta\phi$ like

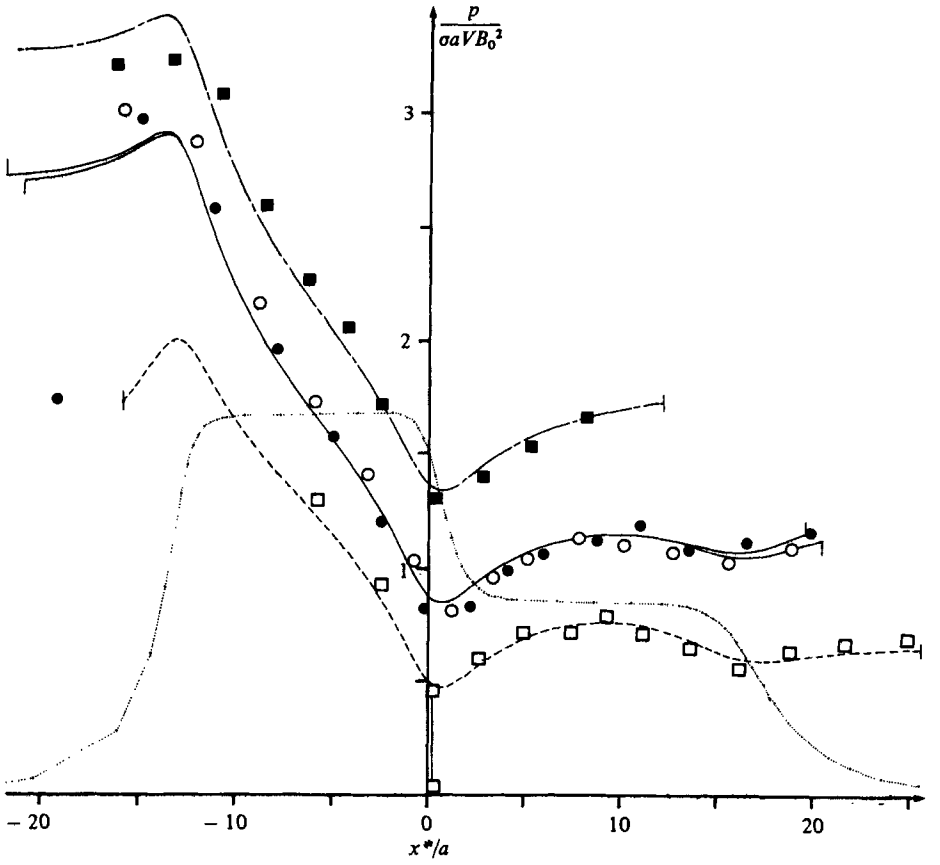

FIGURE 4. Predicted (curves) and measured (points) pressure distributions along duct. Distribution of $B_y = B_y^*/B_0$ at $y = z = 0$ plotted in arbitrary units as ···●···. The ends of the conducting walls are indicated by short vertical lines on the ends of the curves. Near $x^*/a = 0^+$ on the lower distribution, a steady reading could not be obtained; the distance between the pair of points there indicates the range of values measured. (M, N, R): ■·—·■, (509, 47·9, 5406); ●—●, (508, 49·7, 5188); ○—○, (506, 48·4, 5277); □– – –□, (506, 46·4, 5505).

those shown in figure 2. Where $2\lambda B_y > \Delta\phi$ the pressure gradient is negative and where $2\lambda B_y < \Delta\phi$ it is positive.

In all cases it is noticeable that the largest differences between the measured and theoretical distributions occur at the inlet end of the duct. Because the fluid entered the duct as a central jet the flow in the entry region was inevitably unsteady as were the levels of the liquid in the arms of the manometer and so it was impossible to obtain many readings in that region. Even when the inlet was only $3{\cdot}5a$ upstream of the magnet, readings were still difficult to obtain until the flow had travelled a distance of about $10a$ (see lower distribution, figure 4). In the other two cases the entry length appears to be slightly shorter presumably because over the length of duct upstream of the magnet viscous stresses have reduced the velocity of the jet so that the velocity profile is almost uniform whereas in the third case some distance is required for electromagnetic forces to modify the velocity distribution. However, these entry lengths are consistent with those deduced in § 3.3.

Finally, inspection of figure 4 shows that as the length of duct upstream of the

magnet is decreased the net pressure *drop* along it decreases. This is because some of the current which would flow across the duct in the negative z direction upstream of the magnet where $\mathbf{B} = 0$ has to return across the duct in the low field strength region. Therefore the total accelerating force on the fluid increases and hence the total pressure drop along the duct decreases.

4. Conclusions

The results of this study illustrate the gulf between the idealized MHD problems which have been analysed in great detail and the practical MHD problems which the results of the former purport to represent. What at first sight appear to be insignificant departures from an ideal can, in fact, lead to gross differences between predicted and observed behaviour.

Here in § 2.3 an approximate theory has been advanced to allow, principally, the effects of highly – but not perfectly – conducting walls. The experimental results described in § 3 suggests that this theory gives a reasonable description of the integral features of the flow and shows that the predictions of the analysis for perfectly conducting walls given in § 2.2 are misleading. However, the highly conducting wall theory cannot describe the internal structure of the flow – that can only be inferred from the experimental results. Clearly there is room for further experimental and analytical study of this type of problem.

Ideally an analysis is required which caters not only for the present duct with highly, yet finitely, conducting side walls but also for the extreme cases of non-conducting and perfectly conducting walls and all intermediate types. Important factors which must be considered are the form of the magnetic field and hence the variations in M and N along the duct, the length of the conducting walls and any electrical contact between them and, possibly the flows upstream and downstream of the conducting walls. The effect of a three-dimensional non-uniform field and the analogous flows in variable area ducts are also worthy of attention.

Future related experimental investigations must include measurements of velocity profiles (by, for example, hot-film probes) particularly near the conducting walls, to establish how well those qualitative profiles derived from the electric potential distributions represent the actual flow and to form a reliable foundation for explaining its behaviour.

Appendix

The matching condition on the potential distribution, ϕ, at $x = b$ is equivalent to representing the function $f(z)$ defined in (14*b*) by an infinite series of the function ϕ_{w+}, ϕ_f and ϕ_{w-} defined by (14*c–e*) (with $P_k \cosh kx + Q_k \sinh kx$ replaced by a constant coefficient, say A_k) over the range $-\lambda - t_2 < z < \lambda + t_1$. However the functions (14*c*)–(14*e*) are not truly orthogonal over this interval but their first differentials are orthogonal with respect to

$$\Psi_m(z) = \Psi_{w+}(\lambda + t_1' > z > \lambda) + \Psi_f(\lambda > |z|) + \Psi_{w-}(-\lambda > z > -\lambda - t_2'),$$

where m is a root of (15). In the notation of (14*a*),

$$\Psi_{w+} = \sigma' \sin m(\lambda + t_1' - z)/(\sin m\lambda \cos mt_1' + \sigma' \cos m\lambda \sin mt_1'),$$

$$\Psi_f = \cos mz - R_m \sin mz,$$

$$\Psi_{w-} = -\sigma' \sin m(\lambda + t_2' + z)/(\sin m\lambda \cos mt_2' + \sigma' \cos m\lambda \sin mt_2'),$$

so that

$$\int_{-\lambda-t_2'}^{\lambda+t_2'} \Psi_m(z) \frac{\partial}{\partial z}(\phi_{w+} + \phi_f + \phi_{w+})\, dz$$

$$= \int_{\lambda}^{\lambda+t_1'} \Psi_{w+} \frac{\partial \phi_{w+}}{\partial z} dz + \int_{-\lambda}^{\lambda} \Psi_f \frac{\partial \phi_f}{\partial z} dz + \int_{-\lambda-t_2'}^{-\lambda} \Psi_{w-} \frac{\partial \phi_{w-}}{\partial z} dz = \delta_{mk} A_k F_k,$$

where δ_{mk} is the Kronecker delta and F_k is given by (17). It is therefore possible to represent $f'(z)$ by an infinite series of the functions ϕ'_{w+}, ϕ'_f and ϕ'_{w-}; integration of this latter series yields $f(z)$ less an arbitrary constant.

In fact it is possible to find a function ψ_m ($= \int \Psi_m dz$) for which $\int \phi_k \psi_m dz$ is zero unless $m = k$ but the resulting coefficients of the terms in the series do not satisfy Parseval's condition for the series to be a complete representation of $f(z)$ over the interval concerned nor do the terms reduce to those obtained by Vasil'ev & Lavret'ev when $kt' \ll 1$.

The author would like to thank Dr M. D. Cowley and Dr J. C. R. Hunt for supervising the research work which formed the basis of this paper. He would also like to thank Dr E. N. Fox for a discussion about orthogonality relationships and conditions and the referee for his constructive review of the original version of the paper. While carrying out the research the author was supported by grants from the Science Research Council and the Culham Laboratory of the United Kingdom Atomic Energy Authority. The experimental side of the research was financed by Culham Laboratory who also loaned the electromagnet and its motor-generator set and carried out some computational work for the design of its pole pieces. The gear pump used in the experiments was loaned by the Department of Engineering, University of Warwick.

REFERENCES

Holroyd, R. J. 1976 MHD duct flows in non-uniform magnetic fields. Ph.D. dissertation, University of Cambridge.

Holroyd, R. J. 1979 An experimental study of the effect of wall conductivity, non-uniform magnetic fields and variable-area ducts on liquid metal flows at high Hartmann number. Part 1. Ducts with non-conducting walls. *J. Fluid Mech.* **93**, 609.

Holroyd, R. J. & Walker, J. S. 1978 A theoretical study of the effects of wall conductivity, non-uniform magnetic fields and variable area ducts on liquid metal flows at high Hartmann number. *J. Fluid Mech.* **84**, 471.

Hunt, J. C. R. & Ludford, G. S. S. 1968 Three-dimensional MHD duct flows with strong transverse magnetic fields. Part 1. Obstacles in a constant area duct. *J. Fluid Mech.* **33**, 693.

Hunt, J. C. R. & Shercliff, J. A. 1971 MHD at high Hartmann number. *Ann. Rev. Fluid Mech.* **3**, 37.

Hunt, J. C. R. & Stewartson, K. 1965 MHD flow in rectangular ducts. II. *J. Fluid Mech.* **23**, 563.

Kaye, G. W. C. & Laby, T. H. 1973 *Tables of Physical and Chemical Constants (and Some Mathematical Functions)*, 14th edn. Longmans.

Kit, L. G., Peterson, D. E., Platnieks, I. A. & Tsinober, A. B. 1970 Investigation of the influence of fringe effects on a MHD flow in a duct with non-conducting walls. *Magnitnaya Gidrodinamika* **6** (4), 47.

Kulikovskii, A. G. 1968 On slow steady flows of conductive fluid with high Hartmann number. *Izv. Akad. Nauk S.S.S.R. Mekh. Z. i Gaza* **3** (2), 3.

Ludford, G. S. S. & Walker, J. S. 1980 Current Status of MHD duct flows. *Proc. 2nd Bat. Sheva seminar on MHD and turbulence.*

SHERCLIFF, J. A. 1962 *The Theory of Electromagnetic Flow Measurement.* Cambridge University Press.

SHERCLIFF, J. A. 1965 *A Textbook of MHD.* Pergamon Press Ltd.

SHERCLIFF, J. A. 1975 Some duct flow problems at high Hartmann number. *Z. angew. Math. Phys.* **26**, 537.

VASIL'EV, V. F. & LAVRENT'EV, I. V. 1969 Potential distribution in an MHD channel with thin conducting walls. *Magnitnaya Gidrodinamiko* **5** (3), 142.

WALKER, J. S., LUDFORD, G. S. S. & HUNT, J. C. R. 1971 Three-dimensional MHD duct flows with strong transverse magnetic fields. Part 2. Variable area rectangular ducts with conducting sides. *J. Fluid Mech.* **46**, 657.

WALKER, J. S., LUDFORD, G. S. S. & HUNT, J. C. R. 1972 Three-dimensional MHD duct flows with strong transverse magnetic fields. Part 3. Variable area rectangular ducts with insulating walls. *J. Fluid Mech.* **56**, 121.